Competition between α decay and spontaneous fission for heavy and superheavy nuclei

Chang Xu,[1,3,*] Zhongzhou Ren,[1,2,3,4] and Yanqing Guo[1]

[1]*Department of Physics, Nanjing University, Nanjing 210008, People's Republic of China*
[2]*Center of Theoretical Nuclear Physics, National Laboratory of Heavy-Ion Accelerator, Lanzhou 730000, People's Republic of China*
[3]*CPNPC, Nanjing University, Nanjing 210008, People's Republic of China*
[4]*Kavli Institute for Theoretical Physics China, Beijing 100190, People's Republic of China*

(Received 15 June 2008; published 29 October 2008)

We systematically investigate the α-decay and spontaneous fission half-lives for heavy and superheavy nuclei with proton number $Z \geqslant 90$. The α-decay half-lives are obtained by the deformed version of the density-dependent cluster model (DDCM). In the DDCM, the microscopic potential between the α particle and the daughter nucleus is evaluated numerically from the double-folding model with the M3Y interaction. The influence of the core deformation on the double-folding potential is also properly taken into account by the multipole expansion method. The spontaneous fission half-lives of nuclei from ^{232}Th to ^{286}114 are calculated with the parabolic potential approximation by taking nuclear structure effects into account. The agreement between theoretical results and the newly observed data is satisfactory for both α emitters and spontaneous fission nuclei. The competition between α decay and spontaneous fission is analyzed in detail and the branching ratios of these two decay modes are predicted for the unknown cases.

DOI: 10.1103/PhysRevC.78.044329 PACS number(s): 23.60.+e, 25.85.Ca, 21.10.Tg, 27.90.+b

I. INTRODUCTION

It is well known that α decay is an important decay mode for unstable nuclei heavier than the doubly magic nucleus ^{100}Sn. Experiments have shown that there are more than 400 nuclei in the nuclide chart exhibiting the α-decay phenomenon [1]. Alpha decay is considered to be a very powerful tool to investigate the nuclear structure properties of unstable nuclei, especially those approaching the β-stable line and the proton-drip line. More importantly, α decay is also a reliable way to identify the newly synthesized superheavy elements, which is now a hot topic in nuclear physics [2–8]. In addition to α decay, spontaneous fission is another prominent decay type energetically feasible for heavy and superheavy nuclei with proton number $Z \geqslant 90$. It was first predicted by Bohr and Wheeler in 1939 [9] and subsequently observed by Flerov and Petrjak one year later [10]. Since the discovery of spontaneous fission of ^{238}U, a number of actinide nuclei with this type of radioactive decay have been reported in experiments [11]. Recently, the spontaneous fission half-lives of several superheavy nuclei have also been measured by different laboratories [12–17]. Actually, spontaneous fission is also an important limiting factor that determines the stability of newly synthesized superheavy nuclei.

Theoretically, α decay and spontaneous fission share the same underlying mechanism in physics, i.e., the quantum tunneling effect. Extensive studies have been performed to calculate the half-lives of α emitters in the whole nuclide chart, including the superheavy mass region [18–41]. Usually, the α-decay process is considered as an α cluster penetrates the Coulomb barrier after its formation in the parent nucleus. The absolute α-decay width is mainly determined by the product of the α-cluster formation and penetration probabilities. Generally, the α-cluster preformation factor does not change dramatically for most open-shell nuclei and the penetration factor can be well defined by using various effective α-core interactions. As compared to α decay, the situation of spontaneous fission is much more complex and there are large uncertainties existing in the fission process, such as the mass and charge numbers of the two fragments, the number of emitted neutrons, and the released energy, etc. [42]. Thus the full microscopic treatment of such a multidimensional system is extremely difficult.

The aim of this work is to perform detailed studies on both α-decay and spontaneous fission half-lives for heavy and superheavy nuclei. First, we present a new approach for the spontaneous fission half-lives by using the parabolic potential approximation. The most important nuclear structure effects are taken into account in our calculations, such as the strong interaction, the Coulomb interaction, and the isospin effect. By using the new formula derived from the parabolic potential approximation, we systematically calculate the spontaneous fission half-lives of nuclei in the mass region from ^{232}Th to ^{286}114. We also perform a systematic calculation on the α-decay half-lives of nuclei with proton number $Z \geqslant 90$ by the deformed version of the density-dependent cluster model (DDCM). In the DDCM, the microscopic potential between the α particle and the daughter nucleus is evaluated numerically from the double-folding model with the famous M3Y interaction [43]. The penetration probability of the α particle through the deformed Coulomb barrier is obtained by a careful averaging procedure along different orientation angles. The value of the preformation factor in the DDCM is consistent with both the experimental facts and the microscopic calculations. For both α decay and spontaneous fission, the agreement between experimental data and theoretical results is discussed in detail. The competition between these two decay modes is also systematically analyzed. The predicted branching ratios of both α decay and spontaneous fission are

*cxu@nju.edu.cn

given for the unknown cases, which are very helpful for future experiments.

The outline of this article is as follows. In the first and second parts of Sec. II, we present the detailed formulas of the calculations of α-decay and spontaneous fission half-lives, respectively. The numerical results and corresponding discussions are given in Sec. III. Section IV is a brief summary.

II. THEORETICAL FRAMEWORK

A. α decay

First, we briefly introduce the framework of the DDCM [37]. In the DDCM, the α cluster is considered to penetrate the deformed Coulomb barrier after its formation in the parent nucleus. The α-decay width is mainly determined by the product of the α-cluster preformation factor and the penetration probability. The latter one is very sensitive to the details of the α-core interaction, which is the sum of the nuclear potential, the Coulomb potential, and the centrifugal potential [37]

$$V_{\text{Total}}(R,\theta) = V_{\text{N}}(R,\theta) + V_{\text{C}}(R,\theta) + \frac{\hbar^2}{2\mu}\frac{\left(\ell+\frac{1}{2}\right)^2}{R^2}, \quad (1)$$

where R is the separation between the mass center of the α particle and the mass center of the core, θ is the orientation angle of the α particle with respect to the symmetry axis of the daughter nucleus, ℓ is the angular momentum carried by the α particle, and μ is the reduced mass of the α-core system. The nuclear potential is obtained from the double-folding integral of the renormalized M3Y nucleon-nucleon potential with the matter density distributions of the α particle and the daughter nucleus [43]. The Coulomb potential is also obtained from the well-established double-folding model by including the effect of finite size of the α cluster [44]. We assume a spherical α particle interacts with an axially symmetric deformed daughter nucleus. The mass density distribution of the spherical α particle is taken as the widely used Gaussian form [43]. The mass density distribution of the daughter nucleus is a deformed Fermi distribution with standard parameters [37],

$$\rho_2(r_2,\theta) = \rho_0\left\{1+\exp\left[\frac{r_2 - R_0[1+\beta Y_{20}(\theta)]}{a}\right]\right\}, \quad (2)$$

where $R_0 = 1.07\text{A}_d^{1/3}$ fm, $a = 0.54$ fm, and β is the deformation parameter corresponding to the daughter nucleus. In the DDCM, the double-folding potential can be evaluated by the sum of different multipole components,

$$V_{\text{N or C}}(R,\theta) = \sum_{l=0,2,4\ldots} V^l_{\text{N or C}}(R,\theta), \quad (3)$$

and the multipole component of the double-folding potential can be written as [45,46]

$$\begin{aligned} &V^l_{\text{N or C}}(R,\theta)\\ &\quad= \frac{2}{\pi}[(2l+1)/4\pi]^{1/2}\\ &\quad\times \int_0^\infty dk\, k^2 j_l(kR)\tilde{\rho}_1(k)\tilde{\rho}_2^{(l)}(k)\tilde{v}(k)P_l(\cos\theta), \end{aligned} \quad (4)$$

where $\tilde{\rho}_1(k)$ is the Fourier transformation of the density distribution of the α particle and $\tilde{\rho}_2^{(l)}(k)$ is the intrinsic form factor corresponding to the daughter nucleus. $\tilde{v}(k)$ is the Fourier transformation of the effective M3Y nucleon-nucleon interaction or the proton-proton Coulomb interaction. $P_l(\cos\theta)$ is the Legendre function of degree l. The M3Y nucleon-nucleon interaction is given by two direct terms with different ranges, and by an exchange term with a δ interaction [47–49]

$$\begin{aligned} v(s) &= 7999\frac{\exp(-4s)}{4s} - 2134\frac{\exp(-2.5s)}{2.5s} + J_{00}\delta(s)\\ J_{00} &= -276(1-0.005\,E_\alpha/A_\alpha), \end{aligned} \quad (5)$$

where the quantity $|s|$ is the distance between a nucleon in the core and a nucleon in the α particle ($s = R + r_2 - r_1$). E_α is the α-decay energy and A_α is the mass number of the α particle. The depth of the nuclear potential is determined separately for each decay to generate a quasibound state by employing the Bohr-Sommerfeld condition. Once the α-core potential has been determined, the polar-angle-dependent penetration probability of α decay in the deformed version of the DDCM is given by [37]

$$\mathcal{P}_\theta = \exp\left[-2\int_{R_2(\theta)}^{R_3(\theta)}\sqrt{\frac{2\mu}{\hbar^2}|Q_\alpha - V_{\text{Total}}(R,\theta)|}\,dR\right], \quad (6)$$

where $R_2(\theta)$ and $R_3(\theta)$ are the second and third classical turning points for a certain orientation angle θ. The total penetration probability $\mathcal{P}_{\text{Total}}$ is obtained by averaging P_θ in all directions [37]

$$\mathcal{P}_{\text{Total}} = \frac{1}{2}\int_0^\pi \mathcal{P}_\theta \sin(\theta)\text{d}\theta. \quad (7)$$

Finally, the α-decay width in the deformed version of the DDCM is given by [37]

$$\Gamma = \text{P}_\alpha\,\mathcal{F}\,\frac{\hbar^2}{4\mu}\frac{1}{2}\int_0^\pi \mathcal{P}_\theta \sin(\theta)\text{d}\theta, \quad (8)$$

where $\mathcal{F}$ is the normalization factor and P_α is the α-cluster preformation factor in the parent nucleus. The width is then related to the half-life by the well-known relationship $T_{1/2} = \hbar\ln 2/\Gamma$.

B. Spontaneous fission

In principle, the spontaneous fission process is a purely quantum tunneling effect in physics [50,51]. However, there are great difficulties associated with solving such a multidimensional penetration problem microscopically [42]. Usually, one can simplify this problem by using the one-dimensional WKB approximation, in which the penetration probability through the Coulomb barrier is given by

$$\mathcal{P}_{\text{sf}} = \exp\left[-2\int_{R_2}^{R_3}\sqrt{\frac{2\mu}{\hbar^2}[V(R) - Q_{\text{sf}}]}dR\right], \quad (9)$$

where $V(R)$ is the sum of potentials between the two fission fragments and Q_{sf} is the total energy released in the fission process. Here we consider a barrier with the shape of the inverted parabolic potential and $V(R)$ is written as

$$V(R) = V_{\rm top} - \frac{C}{2}(R - R_0)^2, \tag{10}$$

where $V_{\rm top}$ is the height of the Coulomb barrier and C and R_0 are the parameters. By preforming the integral of Eq. (9) with the inverted parabolic potential, the exact expression for the penetration probability $\mathcal{P}_{\rm sf}$ of spontaneous fission can be obtained analytically (the so-called Hill-Wheeler formula) [42],

$$\mathcal{P}_{\rm sf} = \exp\left[-\frac{2\pi(V_{\rm top} - Q_{\rm sf})}{\hbar\omega_f}\right], \tag{11}$$

where ω_f equals $\sqrt{\frac{C}{\mu}}$ and the value of $\hbar\omega_f$ is usually taken as 1.0 MeV. The spontaneous fission half-life $T_{1/2}$ is closely related to the product of frequency factor n and the penetration factor $\mathcal{P}_{\rm sf}$, which can be written as

$$\begin{aligned} T_{1/2} &= \frac{\ln 2}{n\cdot\mathcal{P}_{\rm sf}} = \text{const}\cdot\exp\left[\frac{2\pi(V_{\rm top} - Q_{\rm sf})}{\hbar\omega_f}\right] \\ &= \exp\left[\frac{2\pi c_0}{\hbar\omega_f}\right]\cdot\exp\left[\frac{2\pi(V_{\rm top} - Q_{\rm sf})}{\hbar\omega_f}\right], \end{aligned} \tag{12}$$

where the penetration probability $\mathcal{P}_{\rm sf}$ is expected to be the dominant factor in determining the half-lives of spontaneous fission. The frequency factor n is usually chosen as a constant in calculations. We assume that the height of the Coulomb barrier $V_{\rm top}$ is mainly determined by several important structure properties of spontaneous fission nuclei. The first one is the attractive strong forces between all nucleons, which bind these nucleons together and prevent the nucleus from fissioning into two small fragments. Obviously its total contribution to the stability of nuclei is proportional to the mass number A. The second one is the repulsive Coulomb forces that compete with the attractive strong forces. The magnitude of this term is proportional to Z^2 if we assume the mother nucleus splits into two fragments with equal proton numbers. Actually, a higher order correction of the Coulomb term ($\propto Z^4$) is also needed to describe the transition from asymmetric charge distributions to symmetric charge distributions for different fission nuclei [42]. Third, the isospin effect $(N - Z)^2$ is also very important for the calculations of spontaneous fission half-lives and this term is taken into account in our calculations

$$\begin{aligned} &V_{\rm top} = V_{\rm nuclear} + V_{\rm coulomb} + V_{\rm isospin} \\ &\begin{cases} V_{\rm nuclear} \propto A \\ V_{\rm coulomb} \propto Z_1 Z_2 = \frac{Z}{2}\cdot\frac{Z}{2} = Z^2/4 \\ V_{\rm isospin} \propto (N - Z)^2. \end{cases} \end{aligned} \tag{13}$$

Thus the total expression of $V_{\rm top}$ is given by

$$V_{\rm top} = c_1 A + c_2 Z^2 + c_3 Z^4 + c_4 (N - Z)^2. \tag{14}$$

It should be noted that the physical meaning of each term in Eq. (14) is very clear and the parameters are obtained from the fit to the experimental spontaneous fission half-lives of 45 even-even nuclei from ^{232}Th to ^{286}114. The values of the parameters are $c_0 = -195.09227$, $c_1 = 3.10156$, $c_2 = -0.04386$, $c_3 = 1.40301 \times 10^{-6}$, and $c_4 = -0.03199$.

The systematics of the energy released in fission is directly taken from the nuclear textbook and we do not modify the values of parameters.

$$Q_{\rm sf} = 0.13323\frac{Z^2}{A^{1/3}} - 11.64. \tag{15}$$

By substituting $V_{\rm top}$ and $Q_{\rm sf}$ into Eq. (12), the new expression of spontaneous fission half-lives is given by

$$\begin{aligned} T_{1/2} = \frac{\ln 2}{n\cdot\mathcal{P}_{\rm sf}} = \exp\Bigg\{2\pi\Bigg[&c_0 + c_1 A + c_2 Z^2 + c_3 Z^4 \\ &+ c_4(N - Z)^2 - \left(0.13323\frac{Z^2}{A^{1/3}} - 11.64\right)\Bigg]\Bigg\}. \end{aligned} \tag{16}$$

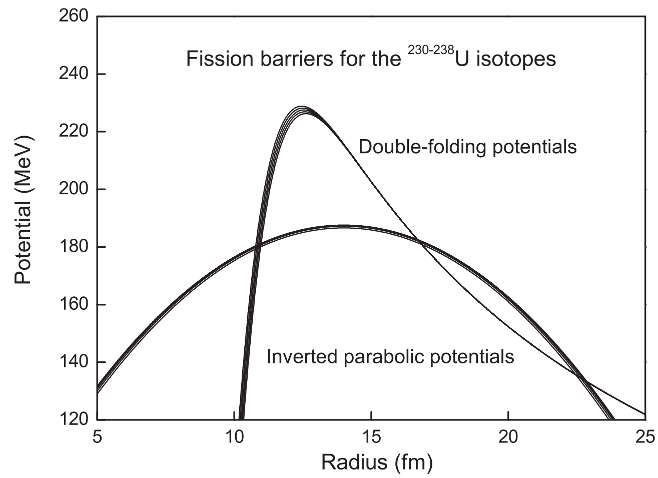

FIG. 1. Fission barriers for the $^{230-238}$U isotopes from the double-folding potential and the inverted parabolic potential.

III. NUMERICAL RESULTS AND DISCUSSIONS

Before we present the detailed theoretical results, it is very interesting to compare the fission barriers from the double-folding potential and the inverted parabolic potential. We choose two representative isotopic chains to illustrate their differences, i.e., the uranium and californium isotopes. In Figs. 1 and 2, we plot the corresponding fission barriers for

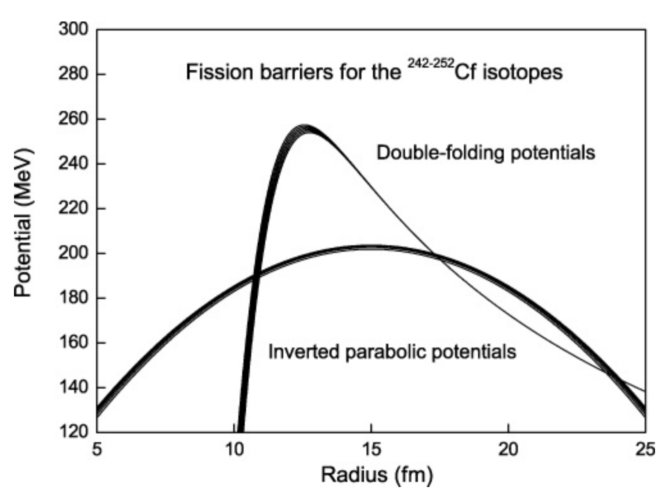

FIG. 2. Fission barriers for the $^{242-252}$Cf isotopes from the double-folding potential and the inverted parabolic potential.

TABLE I. Logarithm of spontaneous fission half-lives of nuclei with proton number $Z = 90$–114 (in years).

Fission	Z	N	$T_{\text{Expt.}}$	$T_{\text{Theo.}}$	Fission	Z	N	$T_{\text{Expt.}}$	$T_{\text{Theo.}}$
^{232}Th	90	142	21.08	21.88	^{250}Fm	100	150	−0.10	−1.57
^{234}U	92	142	16.18	16.03	^{252}Fm	100	152	2.10	−0.92
^{236}U	92	144	16.40	16.56	^{254}Fm	100	154	−0.20	0.98
^{238}U	92	146	15.91	16.38	^{256}Fm	100	156	−3.48	−1.76
^{236}Pu	94	142	9.18	9.71	^{252}No	102	150	−6.54	−6.04
^{238}Pu	94	144	10.68	10.99	^{254}No	102	152	−3.04	−4.65
^{240}Pu	94	146	11.06	11.55	^{256}No	102	154	−4.77	−3.97
^{242}Pu	94	148	10.83	11.40	^{254}Rf	104	150	−12.14	−10.62
^{244}Pu	94	150	10.82	10.54	^{256}Rf	104	152	−9.71	−8.48
^{240}Cm	96	144	6.28	5.02	^{258}Rf	104	154	−9.35	−7.06
^{242}Cm	96	146	6.85	6.33	^{260}Rf	104	156	−9.2	−6.36
^{244}Cm	96	148	7.12	6.92	^{262}Rf	104	158	−7.18	−6.36
^{246}Cm	96	150	7.26	6.80	^{258}Sg	106	152	−10.04	−12.34
^{248}Cm	96	152	6.62	5.96	^{260}Sg	106	154	−9.65	−10.17
^{250}Cm	96	154	4.05	4.41	^{262}Sg	106	156	−9.32	−8.72
^{242}Cf	98	144	−1.33	−1.27	^{264}Sg	106	158	−8.93	−7.98
^{246}Cf	98	148	3.26	2.12	^{266}Sg	106	160	−7.86	−7.96
^{248}Cf	98	150	4.51	2.74	^{264}Hs	108	156	−10.2	−11.02
^{250}Cf	98	152	4.23	2.65	^{270}Ds	110	160	−8.6	−9.46
^{252}Cf	98	154	1.93	1.84	^{282}112	112	170	−10.58	−9.39
^{254}Cf	98	156	−0.78	0.32	^{284}112	112	172	−8.5	−11.43
^{246}Fm	100	146	−6.60	−5.01	^{286}114	114	172	−8.08	−7.12
^{248}Fm	100	148	−2.94	−2.93					

the nuclei $^{230-238}$U and $^{242-252}$Cf, respectively. We note that the fission barriers of the double-folding model are calculated by assuming the two final heavy fragments have almost equal numbers of protons and neutrons, e.g., $^{230}\text{U} \rightarrow {}^{114}\text{Pd} + {}^{116}\text{Pd}$. For the inverted parabolic potential, the fission barriers are well defined by the formula $(c_0' + c_1 A + c_2 Z^2 + c_3 Z^4 + c_4 (N - Z)^2) - \frac{C}{2}(R - R_0)^2$, where the barrier assault frequency is taken as $n = 2.5 \times 10^{20}$ [42]. From Figs. 1 and 2, we can see that the two kinds of fission barriers differ in height and width from each other. As we know, the spontaneous fission half-lives are mainly dependent on the area between the curve of the barrier and the line of fission energy where the range of integral is from the second turning point to the third turning point. For the $^{230-238}$U and $^{242-252}$Cf isotopes, the effective barrier area of the double-folding potential is slightly larger than that of the inverted parabolic model, which may result in a change of the penetration factor by a few orders of magnitude. The microscopic calculations of fission barriers from the double-folding potential are rather difficult because of the uncertainties in the mass and charge numbers of the two fragments. At the same time, it is also very difficult to treat the emitted neutrons in the fission process within the framework of the double-folding potential. By considering the complexity in the fission process, we thus propose a simple approach for the spontaneous fission half-lives by using the parabolic potential.

We have systematically calculated the spontaneous fission half-lives of nuclei in all mass regions from ^{232}Th to ^{286}114 by using the new expression [Eq. (16)]. The detailed results are listed in Table I. In Table I, the first column denotes the spontaneous fission nuclei. The second and third columns are the proton and neutron numbers of nuclei, respectively. The logarithms of experimental and theoretical spontaneous fission half-lives (in years) are listed in the fourth and fifth columns. In Table I, we can see that the experimental spontaneous fission half-lives approximately decrease with the increasing of proton numbers. It is easy to find that the variation of the experimental spontaneous fission half-lives is as high as $10^{21.08}/10^{-12.14} \sim 10^{32}$. Thus it is an extremely difficult task to reproduce the experimental data accurately. However, we can see from Table I that the theoretical spontaneous fission half-lives generally agree well with the experimental results. For many nuclei, the experimental half-lives are reproduced within a factor of 5. For only a few nuclei, the deviation between the experimental and theoretical half-lives is larger than a factor of 10^2. The maximum deviation occurs for the spontaneous fission nucleus ^{252}Fm ($\log_{10}(T_{1/2}^{\text{Expt.}}/T_{1/2}^{\text{Theo.}}) = 3.0$). Such a large deviation is obviously due to the influence of the subshell effect in $N = 152$. This shows that the shell effect is also of vital importance to spontaneous fission nuclei. Our formula can be used to extract the detailed information of subshell closures of the superheavy mass region in further studies. Here the logarithm of average deviations of a total of 45 spontaneous fission nuclei is $S = \Sigma_{i=1}^{i=45} |\log_{10} T_{1/2}^{\text{Expt.}}(i) - \log_{10} T_{1/2}^{\text{Theo.}}(i)|/45 = 0.98$, which correspondences to a factor of 10. This level of agreement is very satisfactory because the spontaneous fission is much more complex than other decay modes such as light cluster radioactivities.

We also performed systematic calculations on the α-decay partial half-lives of heavy and superheavy nuclei using the deformed version of the density-dependent cluster model

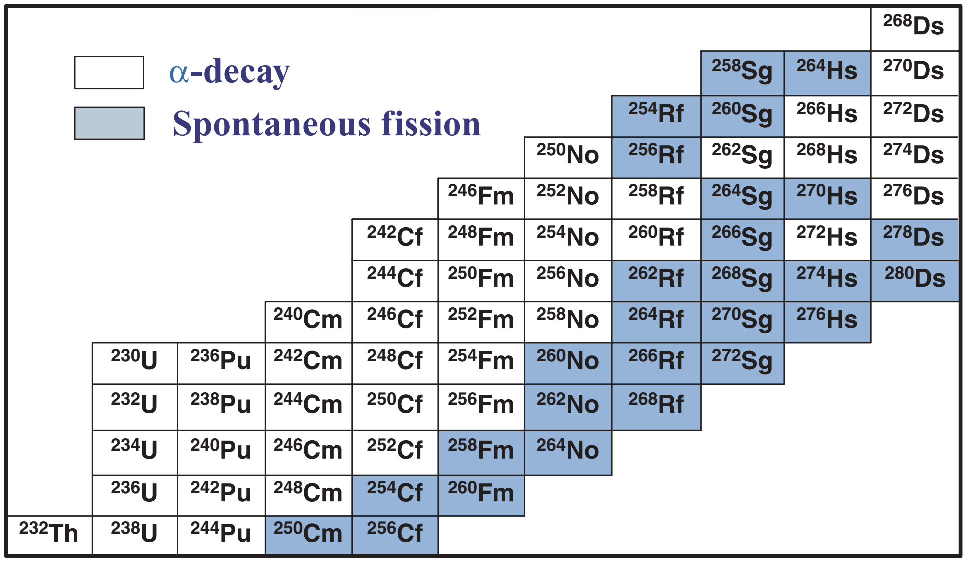

FIG. 3. (Color online) Decay modes of heavy and superheavy nuclei from Th to Ds.

(Th–Ds). In the DDCM, nuclear and Coulomb potentials are microscopically determined in which the input parameters, such as the radius and the diffuseness, are all taken from the classical nuclear textbooks [37]. The depth of the nuclear potential λ is adjusted to reproduce the experimental α-decay energy by applying the Bohr-Sommerfeld condition [37]. The α-cluster preformation factor $P_\alpha = 0.38$ is used for even-even nuclei, which agrees with both the experimental facts and the microscopic calculations [20,23]. The experimental α-decay energies are used in calculations of the DDCM. The small effect of the electron shielding correction on the decay energy Q_α is also included in a standard way [37]. The influence of deformation on α-decay half-lives is taken into account by using theoretical quadrupole deformation from the macroscopic-microscopic model (MM) [52]. The magnitude of α-decay half-lives varies in a wide range and is very sensitive to the α-decay energies. The agreement between experiment and DDCM was found to be quite good for most nuclei (see Ref. [37] for details). The partial α-decay half-lives of 30 even-even nuclei are predicted by using the theoretical α-decay energies [1].

On the basis of the above calculations, we now discuss the competition between α-decay and spontaneous fission decay modes. In Table II, we list the detailed results for both α decay and spontaneous fission of nuclei from Th to Ds. The first column denotes the nuclei. The calculated α-decay partial half-lives are listed in column 2. The symbol * represents the cases in which the experimental α-decay energies are unavailable. The predicted values are used in calculations, which are taken from the NUBASE table of Audi and co-workers [1]. In column 3, the theoretical partial half-lives of spontaneous fission are calculated by our new formula [Eq. (16)]. The experimental and theoretical branching ratios of α decay are given in columns 4 and 5. The last two columns are the experimental and theoretical branching ratios of spontaneous fission, respectively.

We can also see from Table II that the experimental branching ratio of spontaneous fission is very small for lighter actinide nuclei. For example, the intensity of spontaneous fission is only $1.20 \times 10^{-9}\%$ for ^{232}Th, while its α-decay branching ratio is as large as $\sim$100%. Thus the spontaneous fission process is only barely detectable in competition with the more prevalent α-decay mode for these nuclei. However, this is not the case for nuclei with proton number $Z \geqslant 100$. The spontaneous fission begins to compete favorably with the α-particle emission. For some heavy artificial nuclei, spontaneous fission becomes the predominant mode that determines the stability of nuclei. Moreover, the isospin effect $(N - Z)$ is also clearly shown in the experimental branching ratios of heavy and superheavy nuclei. Let us take the uranium isotopic chain $(Z = 92)$ as an example. The spontaneous fission branching ratio of U isotopes increases from $<1.0 \times 10^{-10}\%$ to $5.50 \times 10^{-5}\%$ with the increasing of the neutron number. The same situation also exists for other isotopic chains. Thus the isospin effect is important in the analysis of branching ratios for α decay and spontaneous fission.

Although the experimental branching ratios vary by several orders of magnitude for the isotopic chains, we can see from Table II that the calculated branching ratios of both α decay and spontaneous fission follow the experimental data well. For most cases, the values of the theoretical branching ratios are very close to the experiment results. For example, the uranium isotopic chain (^{230}U–^{238}U) is predicted to mainly undergo α-particle emission (100%), and this agrees with the experimental facts very well. More importantly, the experimental spontaneous fission branching ratios are also satisfactorily reproduced at the same time. Such good agreement is unexpected because one needs to calculate both the α-decay and the spontaneous fission half-lives of these nuclei very accurately. In general, the theoretical branching ratios of both α decay and spontaneous fission are in accordance with the available experiment results with only a few exceptions. It should be noted that the exceptional cases are very helpful in the study of the nuclear structure properties of spontaneous fission nuclei. For instance, the theoretical branching ratios of "doubly magic nucleus" ^{270}Hs are in disagreement with the experimental data. It is concluded that the spontaneous fission half-life of ^{270}Hs is underestimated by our new formula.

TABLE II. Competition between α-decay and spontaneous fission decay modes for nuclei from Th to Ds.

A	T_α(Cal)(s)	T_{sf}(Cal)(s)	B_α(Exp)	B_α(Cal)	B_{sf}(Exp)	B_{sf}(Cal)
^{232}Th	1.2×10^{18}	2.4×10^{29}	100%	100%	1.20×10^{-9}%	5.03×10^{-10}%
^{230}U	4.3×10^{6}	2.1×10^{20}	100%	100%	$< 1.0 \times 10^{-10}$%	2.07×10^{-12}%
^{232}U	5.1×10^{9}	1.9×10^{22}	100%	100%	3.00×10^{-12}%	2.68×10^{-11}%
^{234}U	1.4×10^{13}	3.4×10^{23}	100%	100%	1.60×10^{-9}%	4.23×10^{-9}%
^{236}U	1.4×10^{15}	1.2×10^{24}	100%	100%	9.40×10^{-8}%	1.24×10^{-7}%
^{238}U	3.3×10^{17}	7.6×10^{23}	100%	100%	5.50×10^{-5}%	4.27×10^{-5}%
^{236}Pu	1.2×10^{8}	1.6×10^{17}	100%	100%	1.90×10^{-7}%	7.44×10^{-8}%
^{238}Pu	3.4×10^{9}	3.1×10^{18}	100%	100%	1.90×10^{-7}%	1.09×10^{-7}%
^{240}Pu	3.2×10^{11}	1.1×10^{19}	100%	100%	5.70×10^{-6}%	2.85×10^{-6}%
^{242}Pu	1.8×10^{13}	7.9×10^{18}	100%	100%	5.50×10^{-4}%	2.20×10^{-4}%
^{244}Pu	2.9×10^{15}	1.1×10^{18}	99.88%	99.74%	0.12%	0.26%
^{240}Cm	2.1×10^{6}	3.3×10^{12}	>99.50%	100%	3.90×10^{-6}%	6.39×10^{-5}%
^{242}Cm	1.5×10^{7}	6.7×10^{13}	100%	100%	6.20×10^{-6}%	2.21×10^{-5}%
^{244}Cm	5.4×10^{8}	2.6×10^{14}	100%	100%	1.40×10^{-4}%	2.04×10^{-4}%
^{246}Cm	1.3×10^{11}	2.0×10^{14}	99.97%	99.93%	0.03%	0.07%
^{248}Cm	1.1×10^{13}	2.9×10^{13}	91.61%	71.91%	8.39%	28.09%
^{250}Cm	8.6×10^{12}	8.2×10^{11}	18.00%	8.67%	74%	91.33%
^{242}Cf	3.0×10^{2}	1.7×10^{6}	80.00%	99.98%	⩽0.01%	1.78×10^{-2}%
^{244}Cf	1.4×10^{3}	1.9×10^{8}	≤100%	100%	?%	7.20×10^{-4}%
^{246}Cf	1.1×10^{5}	4.2×10^{9}	100%	100%	2.50×10^{-4}%	2.60×10^{-3}%
^{248}Cf	1.9×10^{7}	1.7×10^{10}	100%	99.89%	2.90×10^{-3}%	1.07×10^{-1}%
^{250}Cf	2.5×10^{8}	1.4×10^{10}	99.92%	98.22%	0.08%	1.78%
^{252}Cf	8.3×10^{7}	2.2×10^{9}	96.91%	96.34%	3.09%	3.66%
^{254}Cf	2.8×10^{9}	6.6×10^{7}	0.31%	2.28%	99.69%	97.72%
^{256}Cf	$3.2 \times 10^{11*}$	3.8×10^{5}	?%	1.18×10^{-4}%	100%	100%
^{246}Fm	1.6×10^{0}	3.1×10^{2}	92.00%	99.48%	8%	0.52%
^{248}Fm	2.5×10^{1}	3.7×10^{4}	93.00%	99.93%	0.1%	0.07%
^{250}Fm	1.0×10^{3}	8.6×10^{5}	>90%	99.88%	6.90×10^{-3}%	0.12%
^{252}Fm	3.7×10^{4}	3.8×10^{6}	100%	99.04%	2.30×10^{-3}%	0.96%
^{254}Fm	7.4×10^{3}	3.3×10^{6}	99.94%	99.78%	0.06%	0.22%
^{256}Fm	1.1×10^{5}	5.5×10^{5}	8.10%	83.43%	91.6%	16.57%
^{258}Fm	$4.8 \times 10^{6*}$	1.8×10^{4}	?%	0.37%	⩽100%	99.63%
^{260}Fm	$1.1 \times 10^{9*}$	1.1×10^{2}	?%	9.98×10^{-6}%	100%	100%
^{250}No	$1.3 \times 10^{-1*}$	2.2×10^{-1}	?%	63.20%	⩽100%	36.80%
^{252}No	2.1×10^{0}	2.8×10^{1}	58.00%	93.24%	19%	6.76%
^{254}No	2.3×10^{1}	7.0×10^{2}	90.00%	96.90%	0.17%	3.10%
^{256}No	1.3×10^{0}	3.4×10^{3}	99.47%	99.96%	0.53%	0.04%
^{258}No	3.5×10^{1}	3.1×10^{3}	?%	98.87%	⩽100%	1.13%
^{260}No	$1.5 \times 10^{3*}$	5.5×10^{2}	?%	26.39%	100%	73.61%
^{262}No	$3.7 \times 10^{5*}$	1.9×10^{1}	?%	5.12×10^{-3}%	100%	99.99%
^{264}No	$8.7 \times 10^{7*}$	1.3×10^{-1}	?%	1.44×10^{-7}%	?%	100%
^{254}Rf	$3.5 \times 10^{-2*}$	7.5×10^{-4}	?%	2.12%	⩽100%	97.88%
^{256}Rf	6.8×10^{-1}	1.0×10^{-1}	0.32%	13.22%	99.68%	86.78%
^{258}Rf	$6.5 \times 10^{-2*}$	2.7×10^{0}	13.00%	97.67%	87%	2.33%
^{260}Rf	$7.3 \times 10^{-1*}$	1.4×10^{1}	?%	95.02%	⩽100%	4.98%
^{262}Rf	$1.5 \times 10^{1*}$	1.4×10^{1}	?%	47.68%	⩽100%	52.32%
^{264}Rf	$2.2 \times 10^{2*}$	2.6×10^{0}	?%	1.17%	?%	98.83%
^{266}Rf	$5.8 \times 10^{4*}$	9.5×10^{-2}	?%	1.64×10^{-4}%	?%	100%
^{268}Rf	$2.9 \times 10^{2*}$	6.7×10^{-4}	?%	2.33×10^{-4}%	?%	100%
^{258}Sg	$2.5 \times 10^{-2*}$	1.5×10^{-5}	?%	0.06%	⩽100%	99.94%
^{260}Sg	4.5×10^{-3}	2.1×10^{-3}	50.%	32.15%	50%	67.85%
^{262}Sg	$3.4 \times 10^{-2*}$	6.0×10^{-2}	⩽22%	64.21%	?%	35.79%
^{264}Sg	$4.5 \times 10^{-1*}$	3.3×10^{-1}	?%	41.84%	?%	58.16%
^{266}Sg	8.2×10^{0}	3.4×10^{-1}	⩽50%	4.01%	⩾50%	95.99%
^{268}Sg	$1.7 \times 10^{2*}$	6.9×10^{-2}	?%	0.04%	?%	99.96%
^{270}Sg	$7.8 \times 10^{-1*}$	2.7×10^{-3}	?%	0.35%	?%	99.65%
^{272}Sg	$3.2 \times 10^{2*}$	2.1×10^{-5}	?%	6.45×10^{-6}%	?%	100%

TABLE II. *(Continued.)*

A	T_α(Cal)(s)	T_{sf}(Cal)(s)	B_α(Exp)	B_α(Cal)	B_{sf}(Exp)	B_{sf}(Cal)
^{264}Hs	5.4×10^{-4}	3.0×10^{-4}	50%	35.60%	50%	64.40%
^{266}Hs	1.8×10^{-3}	9.0×10^{-3}	100%	83.30%	?%	16.70%
^{268}Hs	2.3×10^{-2}*	5.2×10^{-2}	?%	69.18%	?%	30.82%
^{270}Hs	7.8×10^{0}	5.8×10^{-2}	100%	0.74%	?%	99.26%
^{272}Hs	5.9×10^{-3}*	1.3×10^{-2}	?%	68.07%	?%	31.93%
^{274}Hs	2.7×10^{-1}*	5.2×10^{-4}	?%	0.20%	?%	99.80%
^{276}Hs	4.2×10^{1}*	4.2×10^{-6}	?%	1.00×10^{-5}%	?%	100%
^{268}Ds	1.9×10^{-4}*	3.4×10^{-4}	?%	64.27%	?%	35.73%
^{270}Ds	6.4×10^{-5}	1.1×10^{-2}	100%	99.42%	<0.2%	5.80×10^{-1}%
^{272}Ds	6.2×10^{-4}*	6.8×10^{-2}	?%	99.09%	?%	0.91%
^{274}Ds	2.0×10^{-5}*	8.1×10^{-2}	?%	99.98%	?%	0.02%
^{276}Ds	1.5×10^{-3}*	1.9×10^{-2}	?%	92.78%	?%	7.22%
^{278}Ds	5.3×10^{-2}*	8.3×10^{-4}	?%	1.54%	?%	98.46%
^{280}Ds	7.7×10^{0}*	7.1×10^{-6}	?%	9.25×10^{-5}%	100%	100%

As we mentioned above, the spontaneous fission half-life of ^{252}Fm with $N = 152$ is also underestimated by three orders of magnitude, which is due to the absence of the shell effect $N = 152$ in the calculations. Thus this disagreement shows that the subshell closure $N = 162$ also plays an important role in the spontaneous fission process. Further calculations should include the influences of both $N = 152$ and $N = 162$ subshell effects.

For heavier nuclei, the half-lives of α decay and spontaneous fission are difficult to measure and their intensities are still unknown in experiment. This is not surprising because there is often only one or two events of the decay during a long time of observation for the heaviest nuclei. The branching ratios of α decay and spontaneous fission of these nuclei are marked with the symbol ? in the NUBASE table evaluated by Audi and co-workers [1]. In Table II we list the predicted values of branching ratios of these two decay modes for the unknown cases. To show the results more clearly, we also plot in Fig. 3 the possible decay modes of heavy and superheavy nuclei (Th–Ds). In Fig. 3, the white box denotes that α decay is the main decay mode of nuclei, and the blue box represents that the spontaneous fission is the primary decay mode. Again it is seen from Fig. 3 that the unstable nuclei with proton number $Z \geqslant 90$ can undergo either α decay or spontaneous fission. The spontaneous fission decay mode becomes more and more important toward the heaviest side of nuclide chart. The theoretical predictions are useful to estimate the decay mode of newly synthesized superheavy elements before experiment. Also it will be of great interest to compare the theoretical values with the experiment data in the future.

IV. SUMMARY

To conclude, the α-decay and spontaneous fission partial half-lives are systematically calculated for heavy and superheavy nuclei with proton number $Z \geqslant 90$. The α-decay half-lives are obtained by the deformed version of the DDCM with the microscopic double-folding potential. The spontaneous fission half-lives of nuclei are calculated by the parabolic potential approximation with the nuclear structure effects included. A new expression for spontaneous fission half-lives is derived analytically, which works well for the mass region from ^{232}Th to ^{286}114. The physical meaning of each term in this formula is very clear. This new formula can be used to extract the detailed information of the subshell effects in further studies. The competition between α-decay and spontaneous fission decay modes is discussed in detail. It is found that the spontaneous fission becomes more and more important toward the heaviest side of the nuclide chart. Generally, the agreement between experimental and theoretical results is satisfactory for both α decay and spontaneous fission. For the isotopic chains from Th to Fm, the agreement between experimental and theoretical branching ratios is quite good. For the heavier isotopic chains, the experimental branching ratios are reproduced reasonably and the predicted branching ratios are given for the unknown cases by using theoretical decay energies. The branching ratios are very difficult to estimate because one needs to calculate the half-lives of both α decay and spontaneous fission very accurately. The present theoretical predictions on the possible decay modes of heavy and superheavy nuclei will be useful in future experiments.

ACKNOWLEDGMENTS

This work is supported by the National Natural Science Foundation of China (Grants 10535010, 10735010, 10775068, and 10805026), by the 973 National Major State Basic Research and Development of China (Grant 2007CB815004), and by the Research Fund of Doctoral Point (RFDP), No. 20070284016.

[1] G. Audi, O. Bersillon, J. Blachot, and A. H. Wapstra, Nucl. Phys. **A729**, 3 (2003).

[2] S. Hofmann and G. Münzenberg, Rev. Mod. Phys. **72**, 733 (2000).

[3] Yu. Ts. Oganessian *et al.*, Phys. Rev. C **72**, 034611 (2005).
[4] T. N. Ginter *et al.*, Phys. Rev. C **67**, 064609 (2003).
[5] A. Türler *et al.*, Eur. Phys. J. A **17**, 505 (2003).
[6] Z. G. Gan *et al.*, Eur. Phys. J. A **20**, 385 (2004).
[7] K. Morita *et al.*, J. Phys. Soc. Jpn. **76**, 043201 (2007).
[8] C. M. Folden III *et al.*, Phys. Rev. Lett. **93**, 212702 (2004).
[9] N. Bohr and J. A. Wheeler, Phys. Rev. **56**, 426 (1939).
[10] G. N. Flerov and K. A. Petrjak, Phys. Rev. **58**, 89 (1940).
[11] N. E. Holden and D. C. Hoffman, Pure Appl. Chem. **72**, 1525 (2000).
[12] K. E. Gregorich, J. M. Gates, Ch. E. Düllmann, R. Sudowe, S. L. Nelson, M. A. Garcia, I. Dragojević, C. M. Folden III, S. H. Neumann, D. C. Hoffman, and H. Nitsche, Phys. Rev. C **74**, 044611 (2006).
[13] J. Dvorak, W. Brüchle, M. Chelnokov, R. Dressler, Ch. E. Düllmann, K. Eberhardt, V. Gorshkov, E. Jäger, R. Krücken, A. Kuznetsov, Y. Nagame, F. Nebel, Z. Novackova, Z. Qin, M. Schädel, B. Schausten, E. Schimpf, A. Semchenkov, P. Thörle, A. Türler, M. Wegrzecki, B. Wierczinski, A. Yakushev, and A. Yeremin, Phys. Rev. Lett. **97**, 242501 (2006).
[14] D. Peterson, B. B. Back, R. V. F. Janssens, T. L. Khoo, C. J. Lister, D. Seweryniak, I. Ahmad, M. P. Carpenter, C. N. Davids, A. A. Hecht, C. L. Jiang, T. Lauritsen, X. Wang, S. Zhu, F. G. Kondev, A. Heinz, J. Qian, R. Winkler, P. Chowdhury, S. K. Tandel, and U. S. Tandel, Phys. Rev. C **74**, 014316 (2006).
[15] Yu. Ts. Oganessian, V. K. Utyonkov, S. N. Dmitriev, Yu. V. Lobanov, M. G. Itkis, A. N. Polyakov, Yu. S. Tsyganov, A. N. Mezentsev, A. V. Yeremin, A. A. Voinov, E. A. Sokol, G. G. Gulbekian, S. L. Bogomolov, S. Iliev, V. G. Subbotin, A. M. Sukhov, G. V. Buklanov, S. V. Shishkin, V. I. Chepygin, G. K. Vostokin, N. V. Aksenov, M. Hussonnois, K. Subotic, V. I. Zagrebaev, K. J. Moody, J. B. Patin, J. F. Wild, M. A. Stoyer, N. J. Stoyer, D. A. Shaughnessy, J. M. Kenneally, P. A. Wilk, R. Lougheed, H. W. Gaggeler, D. Schumann, H. Bruchertseifer, and R. Eichler, Phys. Rev. C **72**, 034611 (2005).
[16] Yu. Ts. Oganessian, V. K. Utyonkov, Yu. V. Lobanov, F. Sh. Abdullin, A. N. Polyakov, R. N. Sagaidak, I. V. Shirokovsky, Yu. S. Tsyganov, A. A. Voinov, G. G. Gulbekian, S. L. Bogomolov, B. N. Gikal, A. N. Mezentsev, S. Iliev, V. G. Subbotin, A. M. Sukhov, K. Subotic, V. I. Zagrebaev, G. K. Vostokin, M. G. Itkis, K. J. Moody, J. B. Patin, D. A. Shaughnessy, M. A. Stoyer, N. J. Stoyer, P. A. Wilk, J. M. Kenneally, J. H. Landrum, J. F. Wild, and R. W. Lougheed, Phys. Rev. C **74**, 044602 (2006).
[17] Yu. Ts. Oganessian, V. K. Utyonkov, Yu. V. Lobanov, F. Sh. Abdullin, A. N. Polyakov, I. V. Shirokovsky, Yu. S. Tsyganov, G. G. Gulbekian, S. L. Bogomolov, B. N. Gikal, A. N. Mezentsev, S. Iliev, V. G. Subbotin, A. M. Sukhov, A. A. Voinov, G. V. Buklanov, K. Subotic, V. I. Zagrebaev, M. G. Itkis, J. B. Patin, K. J. Moody, J. F. Wild, M. A. Stoyer, N. J. Stoyer, D. A. Shaughnessy, J. M. Kenneally, P. A. Wilk, R. W. Lougheed, R. I. Ilkaev, and S. P. Vesnovskii, Phys. Rev. C **70**, 064609 (2004).
[18] H. Horiuchi, Nucl. Phys. **A522**, 257c (1991).
[19] I. Tonozuka and A. Arima, Nucl. Phys. **A323**, 45 (1979).
[20] P. E. Hodgeson and E. Betak, Phys. Rep. **374**, 1 (2003).
[21] R. G. Lovas, R. J. Liotta, A. Insolia, K. Varga, and D. S. Delion, Phys. Rep. **294**, 265 (1998).
[22] N. Rowley, G. D. Jones, and M. W. Kermode, J. Phys. G: Nucl. Part. Phys. **18**, 165 (1992).
[23] K. Varga, R. G. Lovas, and R. J. Liotta, Phys. Rev. Lett. **69**, 37 (1992).
[24] S. A. Gurvitz and G. Kalbermann, Phys. Rev. Lett. **59**, 262 (1987).
[25] B. Buck, A. C. Merchant, and S. M. Perez, At. Data Nucl. Data Tables **54**, 53 (1993).
[26] P. Mohr, Phys. Rev. C **73**, 031301(R) (2006); Eur. Phys. J. A **31**, 23 (2007).
[27] S. B. Duarte *et al.*, At. Data Nucl. Data Tables **80**, 235 (2002).
[28] B. A. Brown, Phys. Rev. C **46**, 811 (1992).
[29] G. Royer and H. F. Zhang, Phys. Rev. C **77**, 037602 (2008).
[30] P. R. Chowdhury, C. Samanta, and D. N. Basu, Phys. Rev. C **77**, 044603 (2008).
[31] Y. K. Gambhir, A. Bhagwat, and M. Gupta, Phys. Rev. C **71**, 037301 (2005).
[32] R. K. Gupta, M. Balasubramaniam, C. Mazzocchi, M. La Commara, and W. Scheid, Phys. Rev. C **65**, 024601 (2002).
[33] V. Yu. Denisov and H. Ikezoe, Phys. Rev. C **72**, 064613 (2005).
[34] F. R. Xu and J. C. Pei, Phys. Lett. **B642**, 322 (2006).
[35] N. G. Kelkar and H. M. Castañeda, Phys. Rev. C **76**, 064605 (2007).
[36] C. Xu and Z. Ren, Nucl. Phys. **A753**, 174 (2005); Nucl. Phys. **A760**, 303 (2005).
[37] C. Xu and Z. Ren, Phys. Rev. C **73**, 041301(R) (2006).
[38] C. Xu and Z. Ren, Phys. Rev. C **74**, 014304 (2006); Phys. Rev. C **74**, 037302 (2006).
[39] C. Xu and Z. Ren, Phys. Rev. C **75**, 044301 (2007); Phys. Rev. C **76**, 027303 (2007).
[40] D. N. Poenaru, I. H. Plonski, and W. Greiner, Phys. Rev. C **74**,014312 (2006).
[41] D. S. Delion, A. Sandulescu, and W. Greiner, Phys. Rev. C **69**, 044318 (2004); D. S. Delion, S. Peltonen, and J. Suhonen, Phys. Rev. C **73**, 014315 (2006); D. S. Delion, R. J. Liotta, and R. Wyss, Phys. Rev. C **76**, 044301 (2007).
[42] R. Vandenbosch and J. R. Huizenga, *Nuclear Fission* (Academic Press, New York, 1973).
[43] G. R. Satchler and W. G. Love, Phys. Rep. **55**, 183 (1979).
[44] H. J. Krappe, Ann. Phys. **99**, 142 (1976).
[45] M. J. Rhoades-Brown *et al.*, Z. Phys. A **310**, 287 (1983).
[46] M. Ismail, A. Y. Ellithi, and F. Salah, Phys. Rev. C **66**, 017601 (2002).
[47] G. F. Bertsch, J. Borysowicz, H. Mcmanus, and W. G. Love, Nucl. Phys. **A284**, 399 (1977).
[48] A. M. Kobos, B. A. Brown, P. E. Hodgson, G. R. Satchler, and A. Budzanowski, Nucl. Phys. **A384**, 65 (1982).
[49] A. M. Kobos, B. A. Brown, R. Lindsay, and G. R. Satchler, Nucl. Phys. **A425**, 205 (1984).
[50] C. Xu and Z. Ren, Phys. Rev. C **71**, 014309 (2005).
[51] Z. Ren and C. Xu, Nucl. Phys. **A759**, 64 (2005).
[52] P. Möller, J. R. Nix, W. D. Myers, and W. J. Swiatecki, At. Data Nucl. Data Tables **59**, 185 (1995).